Supplementary Information: Sum-Frequency Signals in 2D-Terahertz-Terahertz-Raman Spectroscopy

Griffin Mead,[†] Haw-Wei Lin,[†] Ioan-Bogdan Magdău,[†] Thomas F. Miller III,[†] and Geoffrey A. Blake[*,†,‡]

[†]*Division of Chemistry & Chemical Engineering, California Institute of Technology, Pasadena, California 91125, United States*

[‡]*Division of Geological & Planetary Sciences, California Institute of Technology, Pasadena, California 91125, United States*

E-mail: gab@gps.caltech.edu

2D-TTR Single shot spectrometer

Greater temporal resolution and sensitivity compared to previous research was achieved by developing a single-shot 2D-TTR spectrometer. This technique eliminates scanning of the probe delay line, substantially reducing experimental acquisition time. With the echelon imaging parameters used for this work, each camera acquisition captures 30 ps of molecular response along t_2 at 28 fs resolution. The molecular response along t_1 was captured at an equivalent resolution of 28 fs, while the overall temporal extent of a typical data set spans 30×[5-10] ps ($t_2 \times t_1$). These data therefore represent a $> 10\times$ larger temporal extent compared to previous stage-scan 2D-TTR measurements.[1] Typical acquisition times ranged from a few hours to overnight. (For comparison, the previous stage-scan experiments required around 48 hrs of averaging, over smaller ($t_2 \times t_1$) temporal extents.)

We briefly discuss the overall experimental setup (Supplementary Information Fig. 1), and then provide specific details on the single-shot spectrometer's construction. A 1 kHz Coherent Legend HE regenerative amplifier, seeded with an 80 MHz Coherent Micra oscillator, is used to pump a Light Conversion TOPAS-C optical parametric amplifier (input 3.2 mJ, ∼30% conversion efficiency signal+idler). The 500 μJ 1.4 μm signal output is divided with a 50:50 beam-splitter before illuminating two 6 mm clear aperture DAST THz emitters (4-N,N-dimethylamino-4′-N′-methyl-stilbazolium tosylate, Swiss Terahertz). One OPA pump line is passed off a mechanical stepping delay stage to control the t_1 time delay between the two pump fields. Additionally, one of the 1.4 μm pump line's polarization is rotated 90 degrees so that the THz emission from the two sources can be recombined with a wire-grid polarizer (WGP). Each THz beam is filtered with two 18 THz low-pass filters (QMC Instruments Ltd) after each crystal to remove any residual optical bleed-through. After recombining on the WGP, the THz light is collimated and focused with a series of off-axis parabolic (OAP) mirrors before being focused onto the sample. The sample is held in a 1 mm path length Suprasil cuvette with a 4.6 mm diameter hole drilled in the front face. Over this hole a 5×5 mm clear aperture, 1 μm thick silicon nitride membrane window (Norcada, QX10500F) is

epoxied. This thin membrane minimizes dispersion differences between the THz pump and optical probe fields and also reduces the window response. (Previous works used a sample cuvette with a 1 mm thick quartz or a 300 μm thick diamond window.)

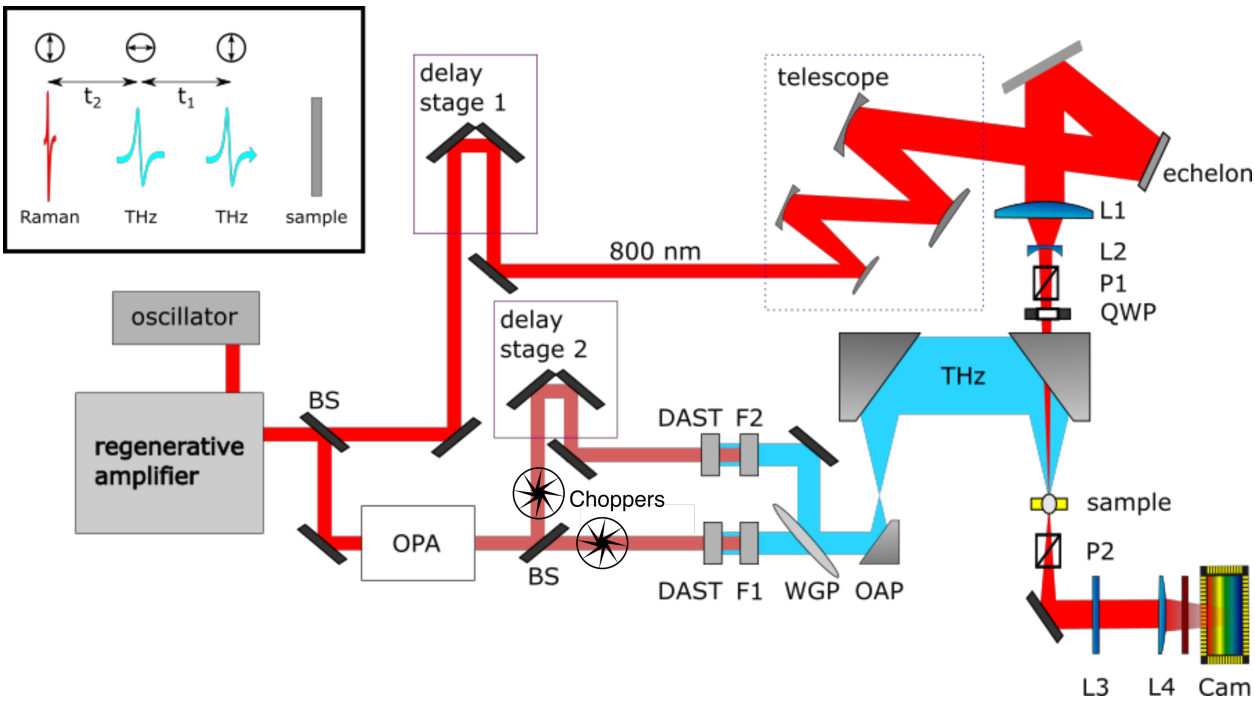

Figure 1: The optical path of the 2D-TTR single-shot spectrometer. Seen in an inset are the polarizations of the two THz pump and 800 nm probe fields, and the experimental time definitions.

The probe line beam conditioning for single-shot acquisition is unchanged from a previous study.[2] Signal photons are detected on an Andor Zyla 5.5 MP sCMOS camera using a pair of crossed 800 nm polarizers with a 10,000:1 extinction ratio (Thorlabs LPVIS050-MP2). The detected signal is sensitive to the anisotropic third order molecular response function $R^{(3)}_{xyxy}(t_1, t_2)$, where the two orthogonal THz pump fields are linearly polarized along the $\vec{x}$ or $\vec{y}$ laboratory axes (with $\vec{z}$ defined as the direction of optical propagation). The same crossed $\vec{x}$ / $\vec{y}$ polarizations hold for the probe and signal fields.

All data and experimental parameters were controlled from a MATLAB GUI purpose-built for the experiments. Each camera acquisition lasted ~800 μs. Within the GUI, the number of acquisitions per average and the number of averages per data set are specified by the user.

For example, typical acquisition settings for a bromoform data set at an arbitrary t_1 time are to collect 5 averages with 2000 shots per average. This requires a total acquisition time of ∼12 seconds, which includes 2 seconds of camera and computational overhead and the 10 seconds of data acquisition. The data set for each average is first collected as a 2000 × 1280 array, with dimensions specified by the number of laser shots captured (2000 in this example), and the 1280 horizontal output pixels (vertically binned) from the camera which capture the time-domain molecular response along t_2 at the fixed t_1 time.

Next, we extract the signal from this data array by performing a FFT on each one of the 1280 rows of data. Each row corresponds to a single point in time t_2 sampled by the probe pulse. These FFTs must be performed carefully to phase relationship of the two THz fields that produce the signal. To do so, we collect several other pieces of data while each average is acquired. First, the REF OUTPUT of the two optical choppers (Thorlabs MC2000/B) that modulate the THz pump fields are recorded on a National Instruments DAQ card. Second, the camera output signal which confirms the start of a series acquisition is digitized by the same DAQ. From these three trigger signals (chopper A phase, chopper B phase, camera acquisition start), we can measure the signal phase of each average and correct for the phase offset. Doing so ensures that every average of every data set at each t_1 time is collected with a single consistent phase, which preserves the overall phase of the 2D signal.

The FFTs are performed by first multiplying each of the 1280 rows of data (each with length n=2000 in this example) with an equal length sinusoidal waveform that incorporates the measured phase offset. The sinusoid frequency is equal to the difference between the two chopper frequencies to exploit the differential chopping of the experiment. Multiplication shifts the desired differential signal to the DC position in the frequency domain FFT output. The DC response from all 1280 channels are then saved as a 1×1280 data array for each average, and are co-added until all averages are collected. In essence, this approach creates a software equivalent to the standard digital lock-in amplifier typically used for collection of multidimensional spectroscopic data.

2D-TTR Sensitivity to IRF

The sensitivity of bromoform's 2D-TTR spectrum to the instrument response function was first noticed as a result of changing the infrared wavelengths that pump the two THz emitters. Initial 2D-TTR experiments used the two orthogonally polarized signal (1.4 μm) and idler (1.8 μm) outputs of the TOPAS-C OPA, each of which pumped one of the DAST crystals. We observed that the majority of the idler line's infrared power was concentrated in a small $\sim$1 mm diameter point within the larger 8 mm diameter beam. As a result of this concentrated point of power, thermal damage was occurring on the face of the DAST crystal. To prevent damage to the emitter crystal from the 1.8 μm line, we split the 1.4 μm signal beam into two halves, rotated one half's polarization to match the idler polarization, and recorded new 2D-TTR data of bromoform. Dramatic differences in bromoform's time (Supplementary Information Fig. 2) and frequency (Supplementary Information Fig. 3) domain responses were observed between the data recorded before and after these changes, drawing our attention to the importance of the IRF in 2D-TTR. SF-RDM analysis of the original 1.4/1.8 μm bromoform data yielded similarly excellent agreement between experiment and simulation.

Halogenated methane purification

Bromoform was purchased from Sigma Aldrich. As received the liquid had a orange hue, indicating some degradation and contamination from water. A simple distillation under nitrogen at 150 degree Celsius was performed to purify the bromoform liquid. NMR analysis indicated complete removal of water. The purified sampled was stored in a round-bottom flask with dry sodium sulfate, under argon in a dark refrigerator. Chloroform was purchased from Sigma Aldrich and used as received.

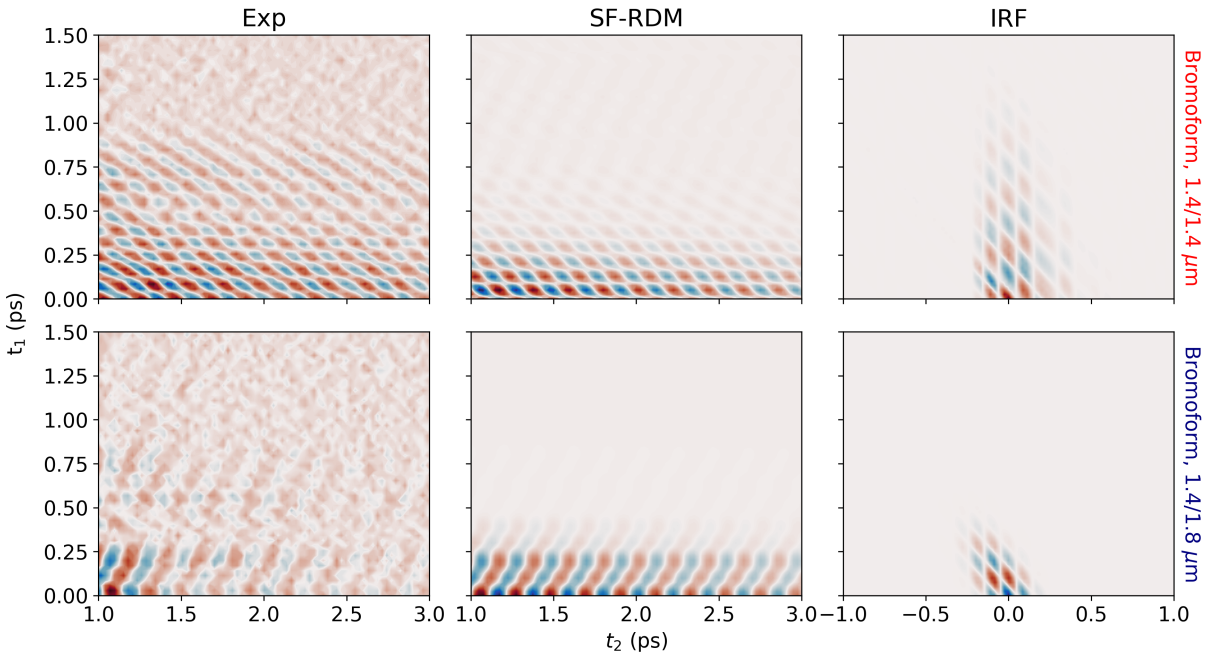

Figure 2: Top and bottom rows compare the experimental (Exp) bromoform time-domain data under two different THz pumping regimes specified on the right hand side of the figure. Slight changes to the emitted THz fields result in different time-domain IRFs. SF-RDM models using the THz electric fields that produce each IRF fully reproduce the experimental data.

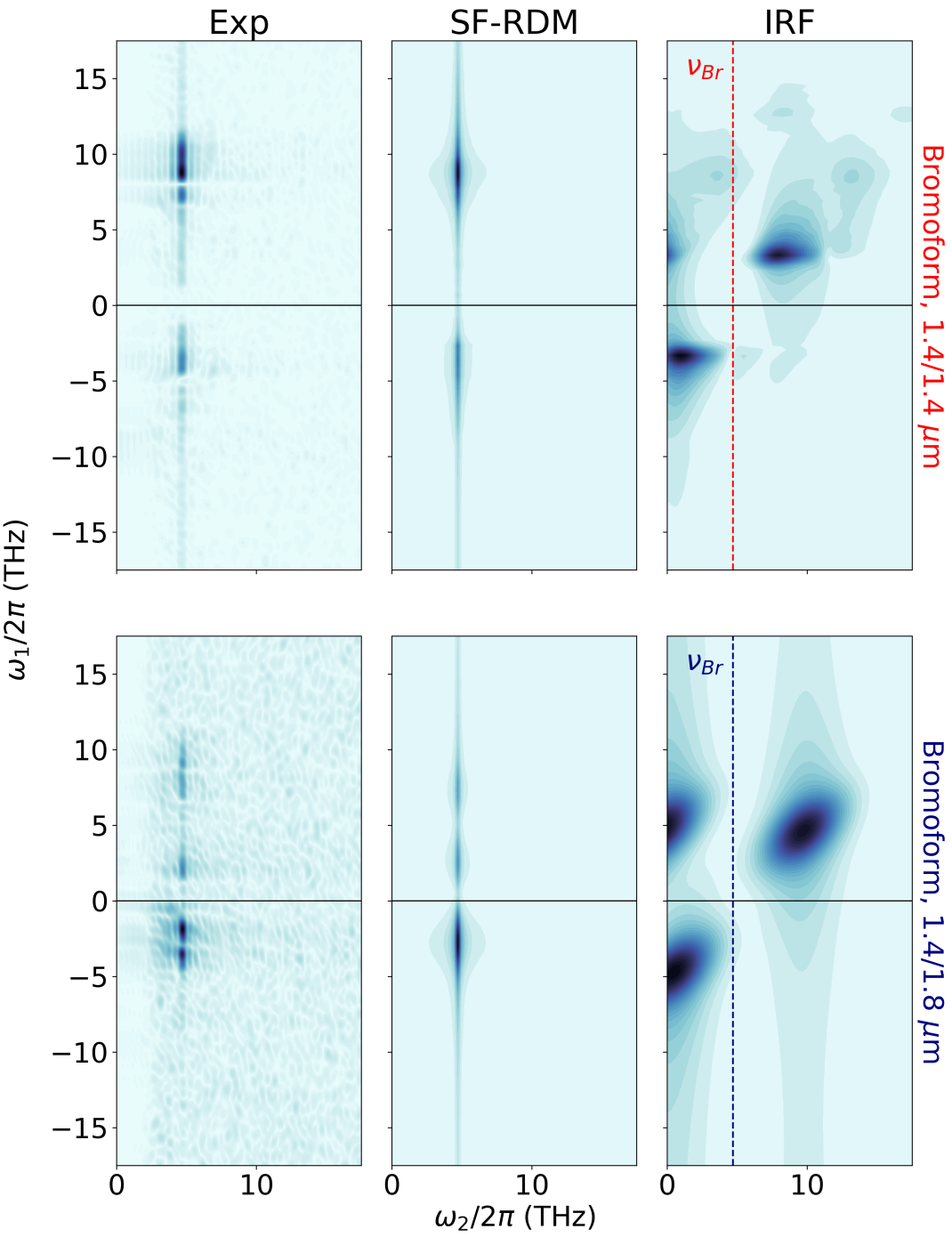

Figure 3: Top and bottom rows compare the experimental (Exp) bromoform frequency-domain data under two different THz pumping regimes specified on the right hand side of the figure. Slight changes to the emitted THz fields result in different frequency-domain IRFs. SF-RDM models with the THz electric fields that produce each IRF reproduce the experimental spectra.

TKE Response of HMs

Terahertz Kerr effect (1D-TKE) measurements of bromoform and chloroform were performed to determine which intramolecular vibrational modes were experimentally observable. The 2D-TTR response of diamond was also measured to gauge the bandwidth of the THz pump field.[1] As shown in Supplementary Information Fig. 4, the THz electric field bandwidth is centered at 4 THz. Bromoform's two Raman-active vibrational modes are observed at 4.7 and 6.6 THz, while the Raman-active vibrational mode in chloroform was observed at 7.8 THz. Note that the orientational (low-frequency) response of both liquids was removed prior to taking the FFT, and only the higher frequency spectral content arising from intra-molecular vibrations are seen in SI Fig. 4.

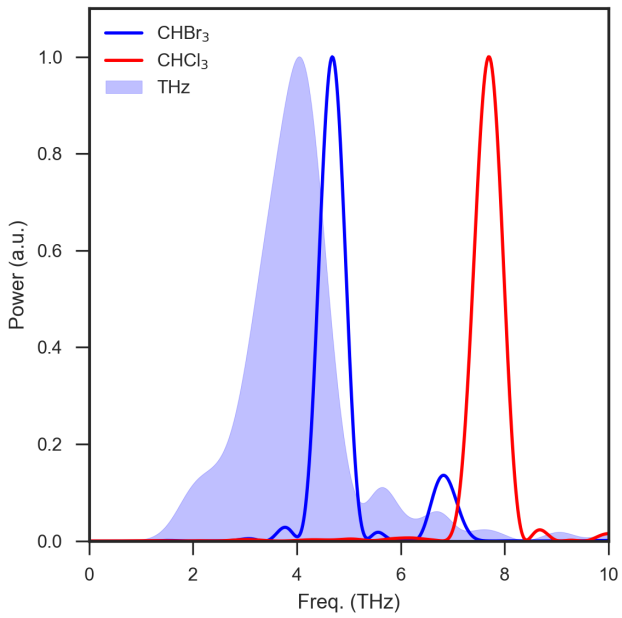

Figure 4: Bromoform and chloroform intramolecular vibrational responses are detected in 1D-TKE measurements. The THz bandwidth of the DAST emission as measured in diamond is shown in blue shading.

THz field modeling

The frequency domain IRF slices at the eigenmode frequencies for halogenated methanes in this study are highly sensitive to small changes in the THz pump pulse shapes. This is especially true for bromoform, whose 4.7 THz eigenmode frequency intersects a region of very low spectral power in the IRF. Near perfect fits to the experimental 2D-TTR spectra of HMs in both the time and frequency domains were obtained by using model THz pulse shapes, which closely resemble the experimental pulse shapes measured in diamond. We believe the use of these model THz pulse shapes is adequate here considering the chromatic nature of the THz focus and the signal-to-noise limitations of the THz bandwidth measured in the diamond 2D-TTR spectra (due to diamond's inherently small $\chi^{(3)}$ constant).

The model THz pulse shapes were obtained with the following process. First, the bandwidths of the two THz pulses were optimized to fit both experimental HM 2D-TTR slices at eigenmode frequencies of bromoform and chloroform. To avoid overfitting, the number of parameters was minimized by assuming a simple asymmetric Gaussian functional form for the THz pulse bandwidth. The time domain IRF is calculated as the product of the THz pulse shapes

$$I(t_1, t_2) = E_1(t_1 + t_2)E_2(t_2)$$

and the Fourier transform of the IRF $\tilde{I}(\omega_1, \omega_2)$ is

$$\tilde{I}(\omega_1, \omega_2) = \tilde{E_1}(\omega_1)\tilde{E_2}(\omega_2 - \omega_1)$$

where $\tilde{E_1}$ and $\tilde{E_2}$ are the bandwidths of the THz pulses. The frequency domain optimization yields only the amplitude spectra, and a phase spectra is still required to uniquely determine the time-domain representation. The hybrid input-output phase retrieval algorithm was used with the experimentally measured THz pulse shapes as targets. Convergence was generally obtained within 100 iterations. The resulting model THz pulses accurately reproduce the observed time and frequency domain results for both HMs, as shown in the main text.

THz pulse shape measurements in general underestimate the available power at higher THz frequencies due to velocity mismatch between the probe (800 nm) and THz pulses, which further supports the increased power above 4 THz for the model pulse shapes.

SF-RDM model

Sum-frequency pathways were not considered in our previous RDM model Hamiltonian[1,3,4]:

$$H(t;t_1) = H_0 - M \cdot [E_2(t-t_1) + E_1(t)] \tag{1}$$

A new Hamiltonian was constructed here, which accounts for the SF process:

$$H(t;t_1) = H_0 - \Pi \cdot [E_2(t-t_1) + E_1(t)]^2 \tag{2}$$

Experimentally, differential chopping of the two THz fields automatically removes the single pulse contributions $\Pi \cdot E_2^2(t-t_1)$ and $\Pi \cdot E_1^2(t)$, so we are left with an effective Hamiltonian of the form:

$$H(t;t_1) = H_0 - \Pi \cdot E_2(t-t_1)E_1(t) \tag{3}$$

The time response is computed as described in our previous work[4], but now it corresponds to an SF signal:

$$S(t_2;t_1) = S_{SF}(t_2;t_1) = Tr(\Pi \cdot \rho(t_2;t_1)) \tag{4}$$

The complete signal S is obtained when E_1 and E_2 are replaced with the fitted pulse shapes, while the molecular response R when E_1 and E_2 are simple δ-functions. All operators are kept linear and harmonic.

References

(1) Finneran, I. A.; Welsch, R.; Allodi, M. A.; Miller, T. F.; Blake, G. A. 2D THz-THz-Raman Photon-Echo Spectroscopy of Molecular Vibrations in Liquid Bromoform. *Journal of Physical Chemistry Letters* **2017**, *8*, 4640–4644.

(2) Mead, G.; Katayama, I.; Takeda, J.; Blake, G. A. An echelon-based single shot optical and terahertz Kerr effect spectrometer. *Review of Scientific Instruments* **2019**, *90*, 053107.

(3) Finneran, I. A.; Welsch, R.; Allodi, M. A.; Miller III, T. F.; Blake, G. A. Coherent two-dimensional terahertz-terahertz-Raman spectroscopy. *Proceedings of the National Academy of Sciences* **2016**, *113*, 6857–6861.

(4) Magdău, I. B.; Mead, G. J.; Blake, G. A.; Miller, T. F. Interpretation of the THz-THz-Raman Spectrum of Bromoform. *The Journal of Physical Chemistry A* **2019**, acs.jpca.9b05165.